Mass accretion rate in the jet-driving symbiotic binary MWC 560

V. D. Marchev[1], R. K. Zamanov[1]
[1] Institute of Astronomy and NAO, Bulgarian Academy of Sciences, Tsarigradsko shose 72, BG-1784 Sofia, Bulgaria
vlad.marchev@gmail.com

(Submitted on 23.08.2023; Accepted on 15.11.2023)

Abstract. We analyze photometric observations of the symbiotic star MWC 560 in B and V bands obtained during the period 1990-2023. We estimate the luminosity and the mass accretion rate of the hot component. We find that the luminosity varies in the range from 200 $L_{\odot}$ to 3000 $L_{\odot}$, corresponding to a mass accretion rate in the range $1 \times 10^{-7} - 2 \times 10^{-6}$ $M_{\odot}$ yr^{-1} (for a 0.9 $M_{\odot}$ white dwarf and distance 2217 pc). The optical flickering disappears at mass accretion rate of about 1×10^{-6} $M_{\odot}$ yr^{-1}, which sets an upper limit for the short-term variability from accreting white dwarf.

Key words: Stars: binaries: symbiotic – accretion, accretion discs – stars: individual: MWC560

1 Introduction

The symbiotic stars are wide binaries with long orbital periods (from 100 days to 100 years), in which material is transferred from a red giant to a white dwarf or a neutron star (Mikołajewska 2012).

The outflow-driving star MWC 560 (V694 Mon) was identified as an emission line object by Merrill & Burwell (1943) in the Mount Wilson observatory spectroscopic surveys. The spectroscopic observations of MWC 560 in 1984 showed that it is an extraordinary symbiotic star with absorption extending out to -3000 km s^{-1} at Hβ, and other Balmer lines (Bond et al. 1984). During the spectroscopic observations at Rozhen Observatory in January - March 1990 the outflow velocities reached 6000 – 7000 km s^{-1}, the absorption was well separated from the emission. Tomov et al. (1990a) proposed that the absorption is caused by jets along the line of sight. The outflow may be a highly-collimated baryon-loaded jet (Schmid et al. 2001) or a wind from the polar regions (Lucy, Knigge & Sokoloski 2018). MWC 560 is considered to be a non-relativistic analog of the quasars because (i) collimated outflow (jets), (ii) the optical emission lines (Balmer lines and FeII lines) are similar to those of the low-redshift quasars (Zamanov & Marziani 2002), and (iii) the absorption lines are similar to the lines of the broad absorption lines quasars (Lucy et al. 2018). The orbital period of the binary is probably $P_{orb} = 1931 \pm 162$ d (Gromadzki et al. 2007), although Munari et al. (2016) proposed that it can be as short as $P_{orb} \approx 330.8$ d.

Here, we analyze B and V photometric observations and estimate the $(B-V)_0$ colour, effective temperature, luminosity and mass accretion rate of the hot component.

2 Observations

We use B and V band data available in the AAVSO database as well as data from Tomov et al. (1990b) and Zamanov et al. (2020). In Fig.1 we plot the AAVSO data for V band (upper panel, green), B band (lower panel, blue). The red plusses are the season average magnitude for the respective observational season (from October to March). We take data for seasons where both B and V measurements are available because both are needed for our further calculations. In Table 1 we present the photometric magnitudes used in this work. Column one is the Julian day of the observation or the season average when using the AAVSO data. Column two and three are the B and V band magnitudes. The other columns are described at the end of Sect. 4.

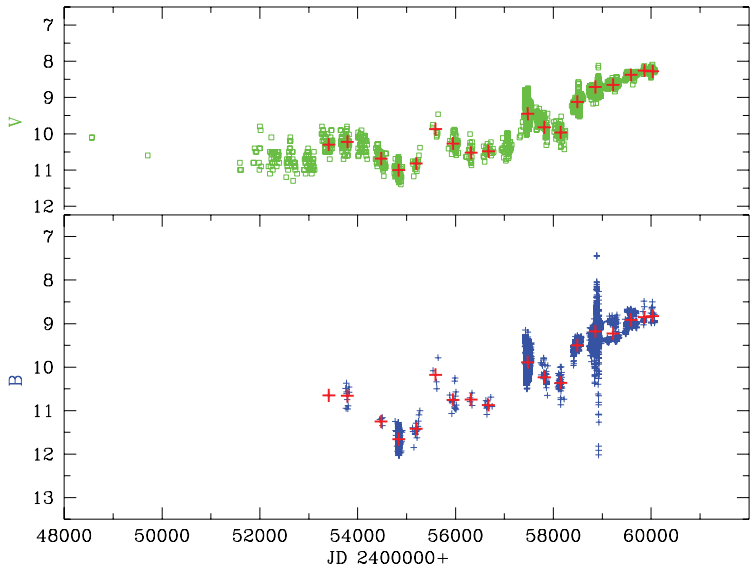

Fig. 1. The AAVSO light curves of MWC 560 from 1987 to 2023 in B and V bands. The red plusses indicate the average value of the magnitude for each observational season.

3 Luminosity of the hot component

To evaluate the brightness of the hot component, we subtract the red giant contribution and make the correction for the interstellar extinction. For the red giant we adopt apparent magnitudes $m_V = 12.25$ and $m_B = 13.94$ (see Sect. 3 in Zamanov et al. 2020). Schmid et al. (2001) estimated interstellar extinction E(B-V)=0.15 mag from the 2200 Å feature. In the light of the NaD absorption and dust maps, the extinction is almost certainly in the range of $0.1 < E(B-V) < 0.2$ (Lucy et al. 2020). Following the mean extinction law

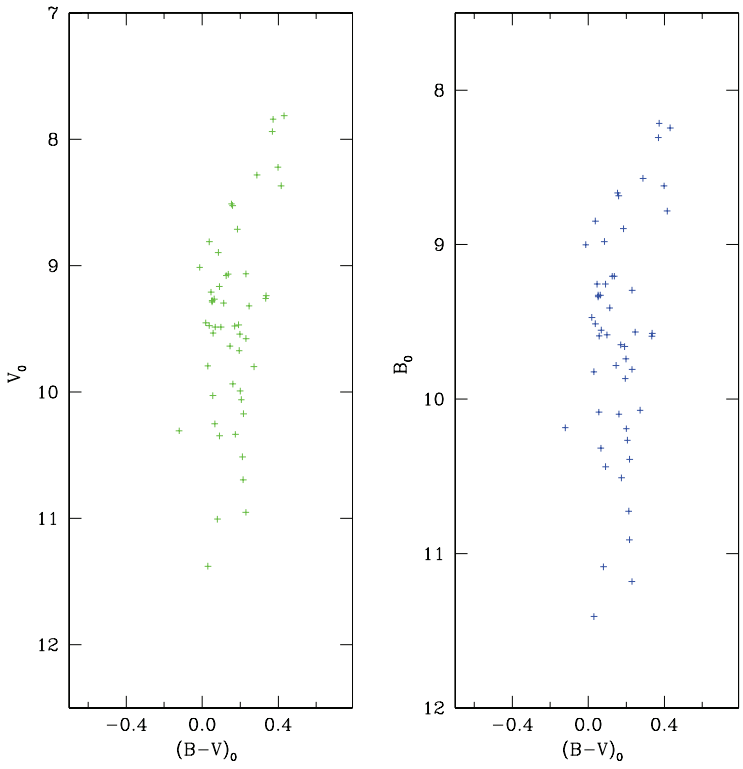

Fig. 2. Dereddened color-magnitude diagram for the hot component of MWC 560. The left panel is V_0 versus $B - V_0$, the right panel is B_0 versus $B - V_0$.

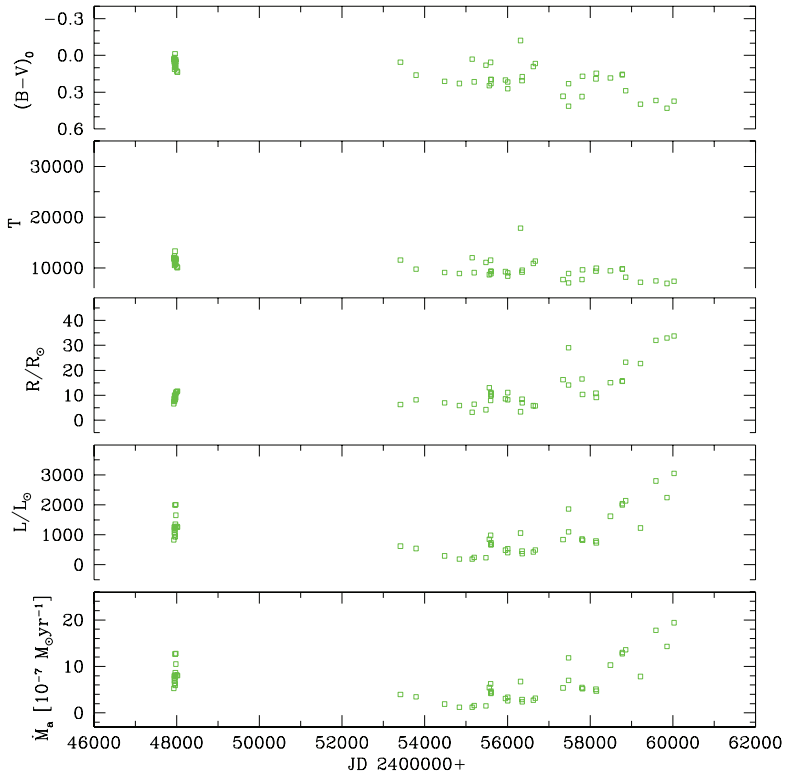

Fig. 3. Evolution of the hot component of MWC 560. From top to bottom dereddened colour $(B\text{-}V)_0$, effective temperature T[K], effective radius in solar units $R/R_\odot$, luminosity in solar units $L/L_\odot$, and mass accretion rate M_a $[10^{-7}\ M_\odot\ yr^{-1}]$ are plotted.

(Eq.1, Eq.3a, Eq.3b in Cardelli, Clayton, & Mathis 1989), we estimate the extinction in B and V bands $A_B = 0.620$ and $A_V = 0.468$, respectively. The model of Bailer-Jones (2021) for the Gaia EDR3 data (Gaia Collaboration et al. 2018), gives a distance $d = 2217$ pc to MWC 560. To estimate the luminosity of the hot component, we applied the following procedure:

1. From the apparent magnitudes we subtract the contribution of the red giant, using the calibrations given in Rodrigo et al. (2018): for Generic Bessell.B filter – effective wavelength 4371.07 Å, zero magnitude star 6.13×10^{-9} erg cm^{-2} s^{-1} Å^{-1}, and for Generic Bessell.V filter – effective wavelength 5477.70 Å, zero magnitude star 3.63×10^{-9} erg cm^{-2} s^{-1} Å^{-1}. This gives the apparent B and V magnitudes of the hot component.

2. We correct them for the interstellar extinction, calculate B_0, V_0, and the dereddened $(B-V)_0$ colour of the hot component (see also Fig. 2).

3. Using $(B-V)_0$ and the calibration for black body (Table 18 in Strayzis 1992), we calculate the effective temperature of the hot component, T_{eff}.

4. Using distance $d = 2217$ pc, and the dereddened magnitudes B_0 and V_0, we estimate the effective radius (R_{eff}) of the hot component. A simple program for the calculation of the radius is given in the Appendix.

5. To derive the optical luminosity of the hot component we use the standard formula:

$$L = 4\pi R_{\rm eff}^2 \, \sigma T_{eff}^4, \tag{1}$$

where $\sigma = 5.67 \times 10^{-5}$ erg cm^{-2} s^{-1} K^{-4} is the Stefan-Boltzman constant.

4 Mass accretion rate onto the white dwarf

The mass accretion rate onto the white dwarf is connected with the optical luminosity:

$$L = \frac{1}{2} \, G \, \frac{M_{wd} \, \dot{M}_a}{R_{wd}}, \tag{2}$$

where G is the gravitational constant, $\dot{M}_a$ is the mass accretion rate, M_{wd} is the mass of the white dwarf, R_{wd} is the radius of the white dwarf. The underlying assumption in this equation is that the disc luminosity is half of the total accretion luminosity. The other half is emitted in UV/X-rays by the boundary layer between the accretion disc and the white dwarf (more details can be found in Chapter 6 of Frank et al. 2012). We adopt for the white dwarf in MWC 560 mass $M_{wd} = 0.9 M_\odot$ and radius $R_{wd} = 6221$ km (Zamanov et al. 2011). Using these values and Eq.2 we calculate the mass accretion rate.

The calculated values of the parameters for each observational data point are presented in Table 1. The column four of the table contains the colour of the hot component, which is used to derive the effective temperature given in column five. Column six is the calculated effective radius in solar radii and column seven is the luminosity in solar luminosity units. Column seven gives the calculated mass accretion rate in units $10^{-7} M_\odot \, yr^{-1}$. All the data from the last 5 columns of Table 1 are presented in Figure 3. In the figure the evolution of the parameters is plotted, from top to bottom, in the order they were obtained – (B-V)$_0$, T_{eff}, R_{eff}, L and $\dot{M}_a$. It is well visible that after JD 2458000 the

R_{eff}, L and $\dot{M}_a$ gradually increase. The optical luminosity goes from around 800 to 3000 $L_\odot$ and the mass accretion rate from 5 to 20 in units $10^{-7} M_\odot yr^{-1}$. The main source of uncertainty comes from the estimation of the red giant's magnitude when subtracting it from the total to get the hot component. The calculated typical uncertainties are $\Delta T_{eff} = \pm 500\ K$, $\Delta R_{eff} = \pm 6 - 8\%$, and $\Delta L = \pm 4\%$. The uncertainty in the luminosity is smaller because the uncertainty for the radius and temperature contribute oppositely. The main source of uncertainty in $\Delta \dot{M}_a$ is coming from the assumptions made in Eq.2 and can be as big as a factor of 1.5.

5 Discussion

In the presented color magnitude diagram (Fig.2), $(B-V)_0$ is in the range from 0.0 to 0.4, which corresponds to black body temperature 7000 - 13000 K. There is only one exception (JD 2456319), which is probably an unusual state, or an observational error, and/or incorrect subtraction of the red giant contribution.

The luminosity of the hot component of MWC 560 is in the range 200 - 3000 $L_\odot$. The luminosities of the hot components in 18 symbiotic stars are estimated using the IUE spectra by Muerset et al. (1991). The luminosity of the hot component of MWC 560 (see Table 1) is similar to the luminosity observed in AG Peg, Z And, SY Mus, AX Per, V443 Her (see Table 5 in Muerset et al. 1991).

We find mass accretion rate onto the white dwarf of MWC 560 in the range $1 \times 10^{-7} - 2 \times 10^{-6}$ $M_\odot$ yr^{-1}. It is considerably higher (two orders higher) than the estimated mass accretion rates in the cataclysmic variables, which are in the range $10^{-11} - 10^{-8}$ $M_\odot$ yr^{-1} (see Table 5 in Pala et al. 2022). Most probably this is because the mass donor (a red giant) in MWC 560 supplies more material than the red dwarfs in the cataclysmic variables.

The accretion-induced variability links young stellar objects, white dwarfs, and black holes (Scaringi et al. 2015). Non-periodic variability on a time scale of ~ 10 minutes (flickering) is observed in many accreting white dwarfs (Bruch 2021). However, the searches for flickering from the accreting white dwarfs in symbiotic stars and related objects (Sokoloski, Bildsten & Ho 2001; Gromadzki et al. 2006; Stoyanov 2012) have shown that the optical flickering is a rarely detectable phenomenon in symbiotic stars. Among more than 300 known symbiotic stars (Akras et al. 2019), only in 12 objects flickering activity is detected till now (a list can be found in Zamanov et al. 2021).

The flickering of MWC 560 is visible in all observations obtained between 1984 and May 2018 (e. g. Lucy et al. 2020 and references therein). The amplitude in U and B bands is in the range 0.1 – 0.4 mag and the detected quasi-periods are from 11 to 160 min (Tomov et al. 1996; Georgiev et al. 2022). The short term variability (flickering) ceased in October 2018 (JD 2458400) and was not detected since then (Marchev et al. 2022, 2023). Our results indicate that the flickering disappears when the mass accretion rate is $\geq 1.10^{-6}$ $M_\odot$ yr^{-1}. We propose two possibilities, when the mass accretion rate exceeds a certain value (1) the accretion disc becomes stable, and no fluctuations in the disc

can be generated, or (2) around the accretion disc forms a "cocoon" (optically thick envelope), which reprocesses the radiation and smears the fluctuations.

Many properties of the flickering can be explained with the fluctuating accretion disc model, where variations in the mass-transfer rate through the disc propagate toward the accreting compact object (Lyubarskii 1997; Kotov et al. 2001, Scaringi et al. 2012). If the first possibility is real, our results set an upper limit ($\approx 10^{-6}$ $M_\odot$ yr^{-1}) above which fluctuations can not be generated in accretion disc around white dwarf.

6 Conclusions

We analyze photometric observations of the jet-driving symbiotic star MWC 560 in B and V bands, obtained during the period 1990-2023. We estimate the luminosity and the mass accretion rate of the hot component. This is done by finding the $(B-V)_0$ colour of the hot component in the range 0.0 to 0.4, which corresponds to effective temperature 7000 - 13000 K. We find that the luminosity varies in the range from 200 $L_\odot$ to 3000 $L_\odot$. Adopting a 0.9 $M_\odot$ white dwarf and distance 2217 pc, we derive mass accretion rate in the range $1.10^{-7} - 2.10^{-6}$ $M_\odot$ yr^{-1}.

The disappearance of the optical flickering corresponds to a luminosity of the hot component 1600 $L_\odot$. Our results indicate an upper limit of the mass accretion rate (of about 1.10^{-6} $M_\odot$ yr^{-1}) above which no flickering can be observed from accretion disc around white dwarf.

Acknowledgments

It is a pleasure to thank the anonymous referee for very thoughtful and stimulating comments, which led to significant improvements of the paper. We acknowledge with thanks the variable star observations from the AAVSO International Database contributed by observers worldwide and used in this research.

References

Akras, S., Guzman-Ramirez, L., Leal-Ferreira, M. L., Ramos-Larios, G., 2019, ApJS, 240, 21
Bailer-Jones, C. A. L., Rybizki, J., Fouesneau, M., Demleitner, M., Andrae, R., 2021, AJ, 161, 147.
Bond, H. E., Pier, J., Pilachowski, C., et al. 1984, BAAS
Bruch, A., 2021, MNRAS, 503, 953
Cardelli, J. A., Clayton, G. C., & Mathis, J. S. 1989, ApJ, 345, 245
Frank, J., King, A., Reine, D., 2012, Accretion Power in Astrophysics, Cambridge University Press
Gaia Collaboration, Brown, A. G. A., Vallenari, A., et al., 2018, A&A, 616, 1
Georgiev, T. B., Boeva, S., Stoyanov, K. A., Latev, G., Spassov, B., Kurtenkov, A., 2022, Bulgarian Astronomical Journal, 37, 62
Gromadzki, M., Mikolajewski, M., Tomov, T., Bellas-Velidis, I., Dapergolas, A., Galan, C., 2006, Acta Astron., 56, 97
Gromadzki, M., Mikołajewska, J., Whitelock, P. A., et al. 2007, A&A, 463, 703
Kotov O., Churazov E., Gilfanov M., 2001, MNRAS, 327, 799
Lucy, A. B., Knigge, C., & Sokoloski, J. L. 2018, MNRAS, 478, 568

Lucy, A. B., Sokoloski, J. L., Munari, U., et al., 2020, MNRAS, 492, 3107
Lyubarskii Y. E., 1997, MNRAS, 292, 679
Marchev, D., Stoyanov, K., Marchev, V., et al., 2022, Acta Scientifica Naturalis, 9, 1
Marchev, D., Yordanova, G., Pavlova, N., et al., 2023, The Astronomer's Telegram, 15906
Merrill, P. W. & Burwell, C. G. 1943, ApJ, 98, 153
Mikołajewska, J., 2012, Baltic Astronomy, 21, 5
Muerset, U., Nussbaumer, H., Schmid, H. M.,& Vogel, M., 1991, A&A, 248, 458
Munari, U., Dallaporta, S., Castellani, F., et al. 2016, New A, 49, 43
Pala, A. F., Gänsicke, B. T., Belloni, D., et al., 2022, MNRAS, 510, 6110
Rodrigo, C., Solano, E., Bayo, A. 2018, IVOA Working Draft 15 October 2012
Scaringi, S., Körding, E., Uttley, P., Groot, P. J., Knigge, C., Still, M., Jonker, P., 2012, MNRAS, 427, 3396
Scaringi, S., Maccarone, T. J., Kording, E., et al., 2015, Science Advances, 1, e1500686
Schmid, H. M., Kaufer, A., Camenzind, M., et al., 2001, A&A, 377, 206
Straižys, V., 1992, Multicolor stellar photometry, Tucson: Pachart Pub. House
Stoyanov, K. A., 2012, Bulgarian Astronomical Journal, 18, 63
Sokoloski, J. L., Bildsten, L., & Ho, W. C. G., 2001, MNRAS, 326, 553
Tomov, T., Kolev, D., Georgiev, L., et al. 1990a, Nature, 346, 637
Tomov, T., Zamanov, R., Antov, A., Georgiev, L., 1990b, IBVS 3466
Tomov, T., Kolev, D., Ivanov, M., et al. 1996, A&AS, 116, 1
Zamanov, R. & Marziani, P. 2002, ApJ, 571, L77
Zamanov, R. K., Boeva, S., Stoyanov, K. A., et al., 2020, Astronomische Nachrichten, 341, 430
Zamanov, R., Gomboc, A., & Latev, G. 2011, Bulgarian Astronomical Journal, 16, 18
Zamanov, R. K., Stoyanov, K. A., Kostov, A., et al., 2021, Astronomische Nachrichten, 342, 952

Table 1. The estimated parameters of the hot component of MWC 560. In the columns are given Julian Day ([a] Tomov et al. 1990, [b] AAVSO data, [c] Zamanov et al. 2021), B and V band magnitudes of MWC 560, estimated $(B-V)_0$ of the hot component, effective temperature, effective radius, optical luminosity, and the mass accretion rate.

JD 2400000+	B [mag]	V [mag]	B-V$_0$	T_{eff} [K]	R_{eff} [$R_\odot$]	L/L$_\odot$	$\dot{M}_a$ [10^{-7} $M_\odot$ yr^{-1}]
47930 [a]	9.823	9.793	0.0294	12018	6.7	829	5.27
47946 [a]	9.338	9.286	0.0517	11605	8.8	1250	7.94
47947 [a]	9.554	9.486	0.0678	11313	8.2	1000	6.35
47948 [a]	9.512	9.475	0.0378	11858	7.8	1088	6.91
47950 [a]	9.471	9.452	0.0190	12330	7.5	1179	7.49
47953 [a]	9.410	9.297	0.1126	10498	9.9	1073	6.82
47954 [a]	9.256	9.166	0.0902	10905	10.0	1273	8.09
47955 [a]	9.328	9.264	0.0635	11391	9.1	1239	7.87
47960 [a]	9.001	9.014	-0.0133	13299	8.4	1994	12.67
47964 [a]	9.585	9.486	0.0988	10749	8.8	930	5.91
47969 [a]	9.256	9.209	0.0465	11700	9.0	1359	8.63
47974 [a]	9.328	9.275	0.0525	11591	8.8	1260	8.00
47982 [a]	8.980	8.896	0.0844	11011	11.2	1655	10.51
47983 [a]	8.848	8.810	0.0376	11862	10.6	2007	12.75
48008 [a]	9.205	9.079	0.1260	10255	11.3	1275	8.10
48016 [a]	9.205	9.068	0.1368	10058	11.7	1260	8.00
53411 [b]	10.084	10.028	0.0561	11525	6.3	624	3.96
53789 [b]	10.098	9.937	0.1611	9736	8.2	543	3.45
54480 [b]	10.726	10.513	0.2124	9095	7.0	297	1.88
54839 [b]	11.181	10.952	0.2297	8879	5.9	194	1.23
55149 [c]	11.408	11.378	0.0303	11995	3.2	192	1.22
55198 [b]	10.911	10.694	0.2162	9048	6.4	250	1.59
55480 [c]	11.086	11.006	0.0801	11089	4.2	239	1.52
55559 [c]	9.566	9.319	0.2469	8664	13.0	854	5.43
55593 [b]	9.591	9.534	0.0573	11504	7.9	981	6.23
55602 [c]	9.808	9.577	0.2309	8864	11.1	686	4.36
55603 [c]	9.867	9.672	0.1948	9315	9.9	659	4.19
55604 [c]	9.740	9.543	0.1977	9279	10.5	740	4.70
55949 [b]	10.192	9.992	0.2002	9248	8.6	488	3.10
56007 [c]	10.072	9.800	0.2726	8342	11.1	535	3.40
56009 [c]	10.390	10.172	0.2179	9026	8.2	403	2.56
56319 [b]	10.186	10.307	-0.1211	17839	3.4	1062	6.75
56354 [c]	10.266	10.061	0.2058	9178	8.4	454	2.88
56356 [c]	10.510	10.335	0.1751	9561	7.0	369	2.34
56625 [c]	10.438	10.347	0.0914	10884	5.8	428	2.72
56675 [b]	10.318	10.252	0.0658	11349	5.8	496	3.15
57344 [c]	9.592	9.258	0.3342	7715	16.3	843	5.36
57478 [b]	9.295	9.065	0.2303	8871	14.1	1101	6.99
57480 [c]	8.783	8.368	0.4153	7039	29.1	1863	11.83
57806 [c]	9.574	9.238	0.3367	7694	16.5	858	5.45
57816 [b]	9.649	9.478	0.1712	9610	10.3	816	5.19
58142 [c]	9.660	9.468	0.1918	9352	10.8	799	5.07
58151 [b]	9.782	9.637	0.1457	9929	9.2	734	4.66
58491 [b]	8.897	8.712	0.1849	9439	15.1	1620	10.29
58778 [c]	8.666	8.512	0.1540	9825	15.6	2042	12.97
58781 [c]	8.684	8.524	0.1604	9745	15.7	1999	12.70
58858 [b]	8.571	8.283	0.2882	8148	23.2	2136	13.57
59221 [b]	8.620	8.221	0.3986	7178	22.7	1230	7.81
59589 [b]	8.307	7.938	0.3687	7427	32.0	2797	17.77
59860 [b]	8.244	7.813	0.4312	6930	33.0	2246	14.27
60032 [b]	8.214	7.841	0.3731	7391	33.8	3054	19.40

Appendix

Here we give a simple program used for the calculation of the radius of a black body located at a distance 2217 pc, with temperature 10000 K, dereddened B band magnitude 11.0. This program uses the IDL Astronomy Users Library (https://idlastro.gsfc.nasa.gov/):

```
wave=4378.12
mag3= 11.0
T1= 10000.0
R= 10.0
d1= 2217.0*3.0857e18 R1= R * 6.96e10
flu1= R1/d1*R1/d1 * planck(wave,T1)
mag1=-2.5*alog10(flu1/6.293e-9)
dmag= mag1 - mag3
R3 = R*sqrt(10^(dmag/2.5))
print, R, mag1, mag3
print, R3
```

In the above program are used 1 pc= 3.0857×10^{18} cm, effective wavelength of the B band 4378.12 Å, and flux of zero magnitude star in B band 6.293×10^{-9} erg cm^2 s^{-1} Å^{-1}. The program uses an initial value of R given by hand and it calculates the flux with the built in Plank function for the coresponding wavelength and temperature. Finally it derives the Radius R3 based on the difference in the magnitude.